8

EFFICIENCY IMPROVEMENT OF CdS AND CdSe QDSSCs BY TiO_2 SURFACE TREATMENT[*]

8.1 Introduction

In general, there are a few notable approaches for solar cell performance improvement, namely QD deposition method, choice of electrolyte, and type of counter electrode materials. Another method is surface treatment of the photoanode electrode [1]. This approach is aimed to reduce the resistance in the photoanode structure so that charge can be transferred to the conducting glass substrate efficiently. It is also important to reduce the charge recombination at the photoanode/electrolyte interface. Some of the strategies used are passivating the photoanode surface with ZnS [2], using different sizes of TiO_2 nanoparticles [3], depositing a scattering layer [4] and treatment with titanium chloride, $TiCl_4$ [5]. While some methods work well in DSSC, they may not produce the same positive effect in QDSSC.

---

[*] Portion of this chapter were published in: Jun, H.K., Careem, M.A., & Arof, A.K. (2014). Efficiency improvement of CdS and CdSe quantum dot-sensitized solar cells by TiO_2 surface treatment. *Journal of Renewable and Sustainable Energy,* 6, 023107.

In this work, few methods of surface treatment were employed in CdS and CdSe QDSSCs. The solar cells were first passivated with ZnS layer. Then a scattering layer was introduced into the structure. By varying the TiO_2 film thickness, a positive effect in performance was observed. A brief treatment of TiO_2 film with $TiCl_4$ was then studied. Finally a new way of QD deposition was studied i.e. doping with optically active transition metal ions.

CdS and CdSe QD-sensitized TiO_2 electrodes were prepared based on optimized parameters as reported in Chapter 4. ZnS layer and polysulfide electrolyte for CdS QDSSC was prepared according to procedures in Chapter 3. For CdSe QDSSC, the electrolyte was prepared based on the result in Chapter 5.

8.2 Results and discussion

8.2.1 Surface treatment effect in QDSSC

The CdS QDSSC performance with various photoanode structures is presented in the *J-V* curves as shown in Figure 8.1. The corresponding performance parameters are tabulated in Table 8.1. With basic photoanode structure in CdS QDSSC, an efficiency of 1.06% was recorded. Photocurrent density of 6.09 mA/cm^2 was obtained for the same cell. However, the performance can be improved with the deposition of ZnS overlayer [2,6]. The efficiency of the cell with TiO_2/CdS/ZnS photoanode structure increased by 35% to 1.43%. The improvement was mainly driven by the improved photocurrent density where it registered a 64% increment. This positive effect is attributed to the better charge transfer in the photoanode structure where the electron

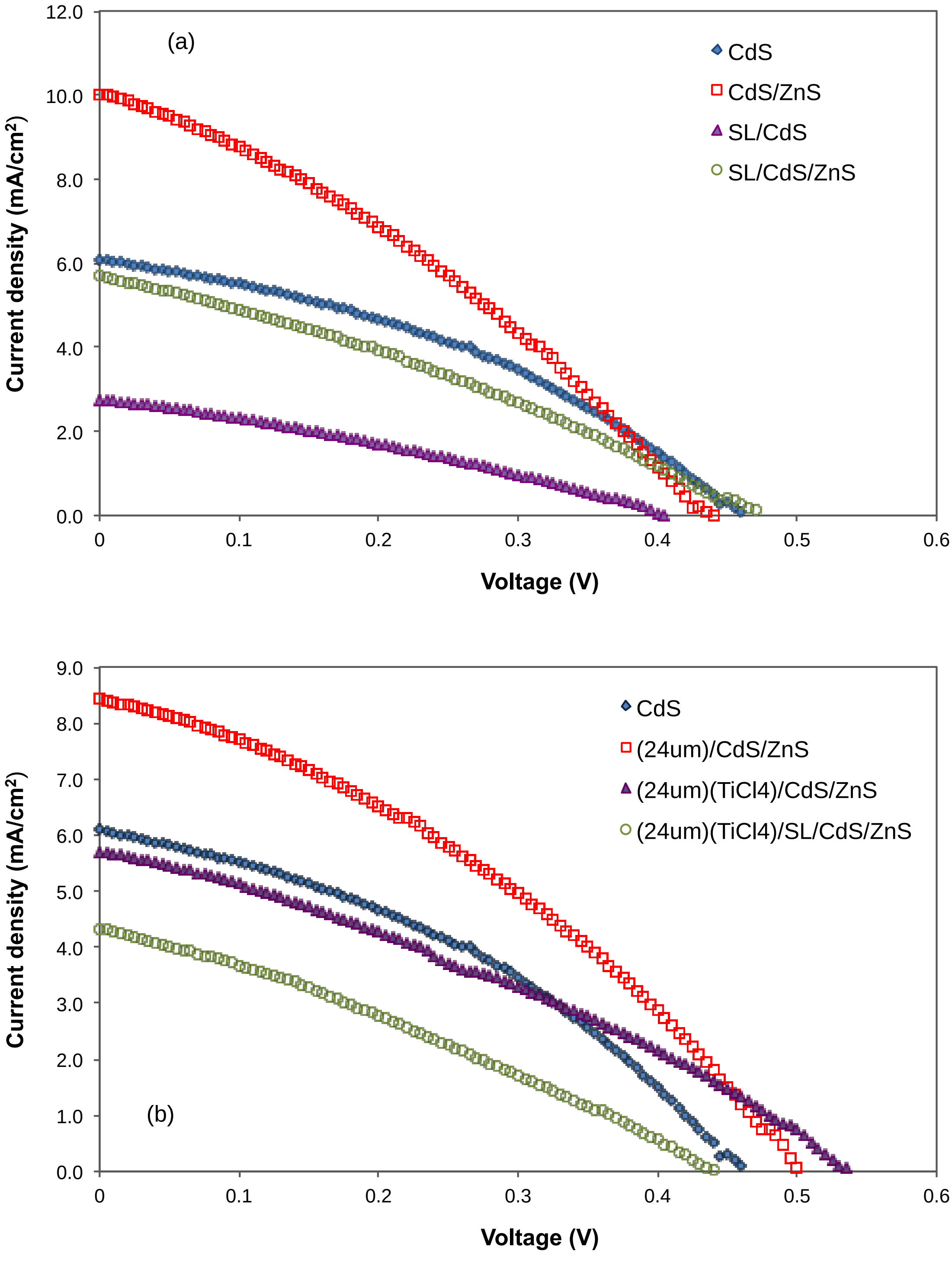

Figure 8.1. *J-V* curves for CdS QDSSC with various photoanode structures. (a) Nominal TiO_2 thickness, and (b) increased TiO_2 thickness. “SL” denotes the scattering layer, “24um” indicates a thicker TiO_2 layer applied and “TiCl4” indicates treatment with $TiCl_4$.

recombination has been suppressed by the ZnS passivation layer. At the same time, ZnS also reduces the effect of photocorrosion on the QDs. [2,7]. The same improvement is also observed in CdSe QDSSC. CdSe QDSSC performance results are shown in Figure

8.2 with the corresponding data tabulated in Table 8.2. A basic CdSe QDSSC structure had an efficiency of 1.41%. With ZnS passivation layer added on top of the CdSe-sensitized TiO_2 film, the efficiency improved to 1.48%. Photocurrent density also increased from 6.80 to 8.36 mA/cm^2. The addition of ZnS layer is thought to facilitate the charge transfer rate from QD to TiO_2 as suggested by Guijarro *et al.* [7]. Even with the addition of ZnS layer, the cascade-type energy band structure of the photoanode is still prevalent as this structure is favourable for the hole transport [8]. The proposed energy band structure alignments for both QDSSC are illustrated in Figure 8.3.

Table 8.1. Performance parameters of CdS QDSSCs with various photoanode structures.

	J_{SC} (mA/cm^2)	V_{OC} (V)	FF (%)	η (%)
TiO_2/CdS	6.09	0.46	38.0	1.06
TiO_2/CdS/ZnS	10.00	0.44	32.5	1.43
TiO_2/SL/CdS	2.76	0.41	31.0	0.35
TiO_2/SL/CdS/ZnS	5.70	0.47	31.0	0.83
TiO_2(2x)/CdS/ZnS	8.43	0.50	35.0	1.48
TiO_2(2x)($TiCl_4$)/CdS/ZnS	5.71	0.54	32.0	0.98
TiO_2(2x)($TiCl_4$)/SL/CdS/ZnS	4.33	0.44	30.0	0.57

In DSSC, it is common to apply a scattering layer on top of the TiO_2 porous structure [9-12]. In general, the scattering layer consists of larger size of TiO_2 nano-particles. Typical size ranges from 200-400 nm. The scattering layer helps to reflect the unabsorbed light within the TiO_2 porous structure. This effect further enhances the light harvesting especially in the near IR region. Although scattering layer has been beneficial in DSSC, there is not much report on QDSSC. In the work by Hossain *et al.* [4], addition of scattering layer did help to improve the performance of CdS and CdSe co-sensitized solar cell. In this study, TiO_2 paste with particle size > 200 nm was spread on top of the sintered TiO_2 film. The electrode was then sintered at 450°C for 30 min before subjected to QD deposition. In CdS QDSSC with scattering layer, the performance of the cell deteriorated compared to that without the scattering layer (refer to result in Figure 8.1 and Table 8.1). It has an efficiency of 0.35%, which registers a lost of 67% compared to the normal CdS QDSSC. Even with the ZnS passivation, the performance is still inferior. The efficiency of such cell is 0.83% with an increased photocurrent density of 5.70 mA/cm^2. Again, the improvement is mainly contributed by the role of ZnS layer which suppresses the electron recombination. On the other hand, the negative effect of the scattering layer in CdSe QDSSC is not that great (refer Figure 8.2 and Table 8.2). CdSe QDSSC with scattering layer has an efficiency of 1.37%, just slightly lower than the normal cell structure (1.41%). Although the photocurrent density improved slightly, this effect is offset by the lower fill factor value. With the addition of ZnS layer, the efficiency improved to 1.41% but with a slight decrease in photocurrent density. The negative effect of scattering layer in CdS QD is not well understood yet. It could be due to more electron recombination at the TiO_2/electrolyte interface as CdS QD may not grow effectively on the larger TiO_2 crystal surface.

TiO_2 film thickness also influences the performance of the solar cell. Efficient DSSC is obtained when the TiO_2 thickness is at optimum which is around 11 μm [10,13]. The low thickness is favoured for the fast and smooth charge collection from dye to TiO_2 [14,15]. In QDSSC, different TiO_2 thickness also produces different cell performance. Coincidently, the high efficiency QDSSC had TiO_2 thickness around 12 μm [16,17]. In this study, a single Scotch tape used during the TiO_2 doctor-blading process produced a film thickness about 11.9 μm as observed from the FESEM cross sectional image as shown in Figure 8.4. With double Scotch tape, a TiO_2 film thickness of 23.6 μm was obtained. As reported above, CdS QDSSC with 11.9 μm of TiO_2 thickness has an efficiency of 1.43% (with ZnS passivation layer). With thicker TiO_2 film, the performance improved by a small 3.5% to 1.48%. This improvement is largely driven by higher open-circuit voltage and fill factor values. In CdSe QDSSC, a thicker

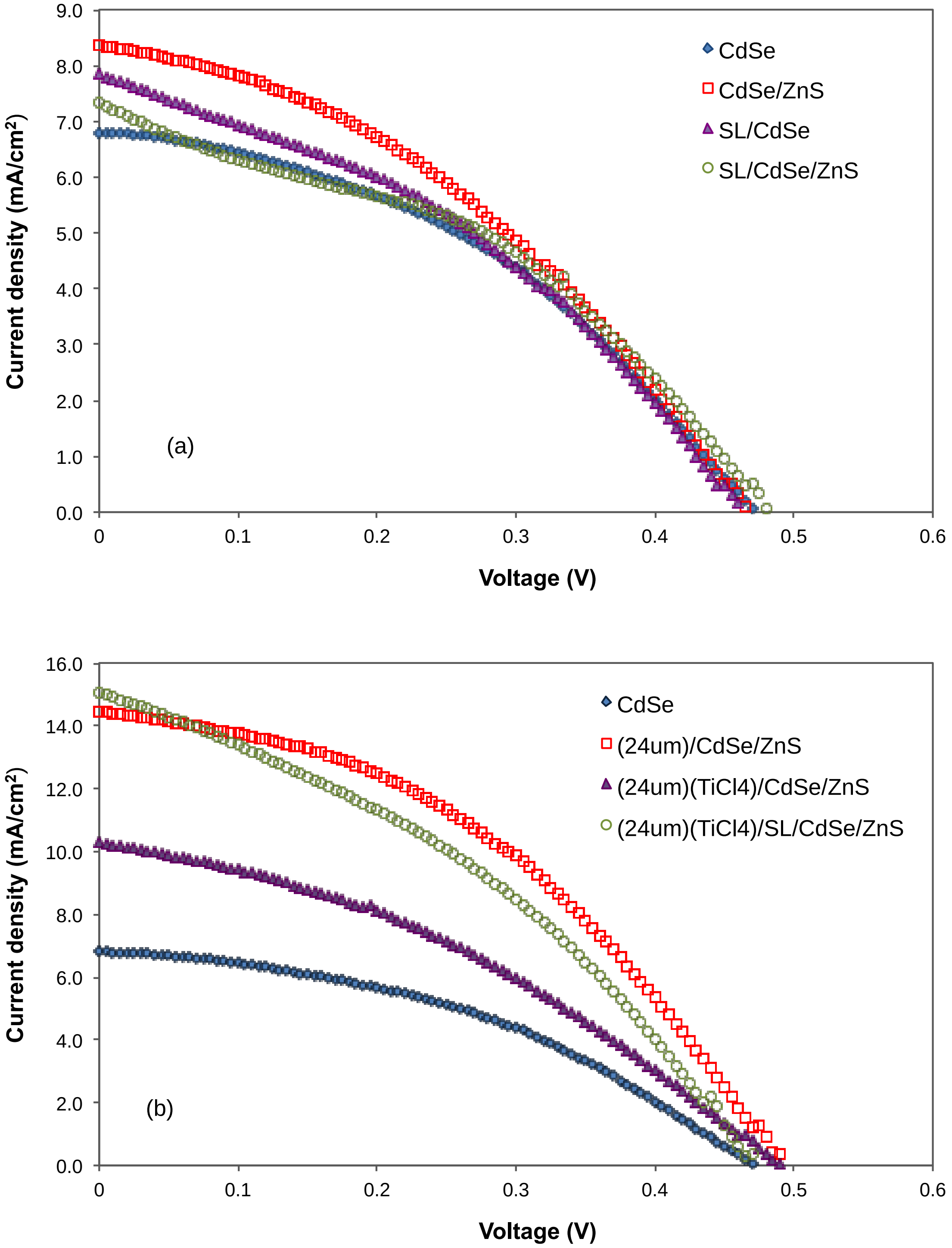

Figure 8.2. *J-V* curves for CdSe QDSSC with various photoanode structures. (a) Nominal TiO_2 thickness, and (b) increased TiO_2 thickness. “SL” denotes the scattering layer, “24um” indicates a thicker TiO_2 layer applied and “TiCl4” indicates treatment with $TiCl_4$.

TiO_2 film results in a significant improvement where the cell efficiency is 3.05%. This is more than double compared to the normal CdSe QDSSC with ZnS passivation layer. This high performing CdSe QDSSC has photocurrent density of 14.16 mA/cm^2 and better open-circuit voltage of 0.49 V. In both CdS and CdSe QDSSC, the high performance observed with thicker TiO_2 film indicates more photocurrent transfer due to more amount of QDs deposited on the enlarged surface area of the TiO_2 particles. The high performance is also helped by the effective ZnS passivation layer as explained previously.

Table 8.2. Performance parameters of CdSe QDSSCs with various photoanode structures.

	J_{SC} (mA/cm^2)	V_{OC} (V)	FF (%)	η (%)
TiO_2/CdSe	6.80	0.47	44.0	1.41
TiO_2/CdSe/ZnS	8.36	0.47	38.0	1.48
TiO_2/SL/CdSe	7.85	0.46	38.0	1.37
TiO_2/SL/CdSe/ZnS	7.35	0.48	40.0	1.41
TiO_2(2x)/CdSe/ZnS	14.46	0.49	43.0	3.05
TiO_2(2x)($TiCl_4$)/CdSe/ZnS	10.28	0.49	36.0	1.81
TiO_2(2x)($TiCl_4$)/SL/CdSe/ZnS	15.04	0.44	39.0	2.55

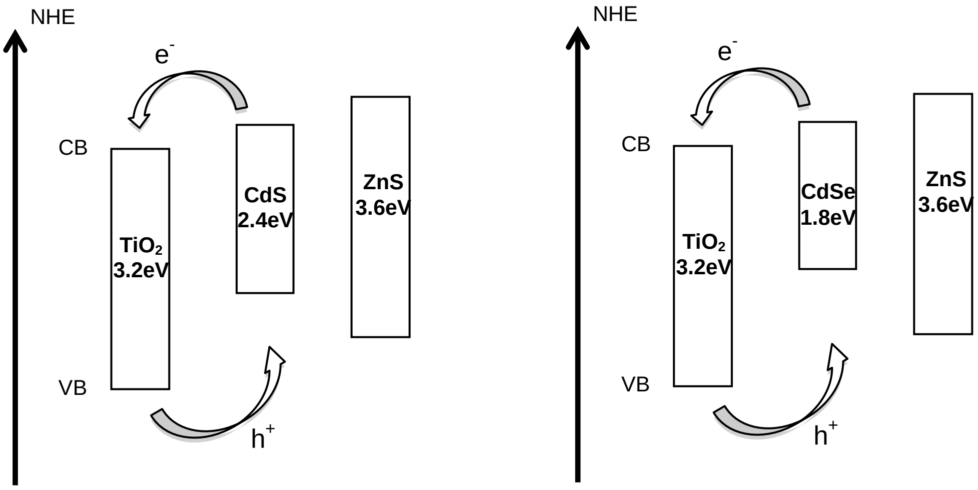

Figure 8.3. Proposed energy band structure alignment of TiO_2/CdS/ZnS and TiO_2/CdSe/ZnS interface at conductive state. The energy levels are referenced to NHE scale. VB and CB are valence band and conduction band, respectively.

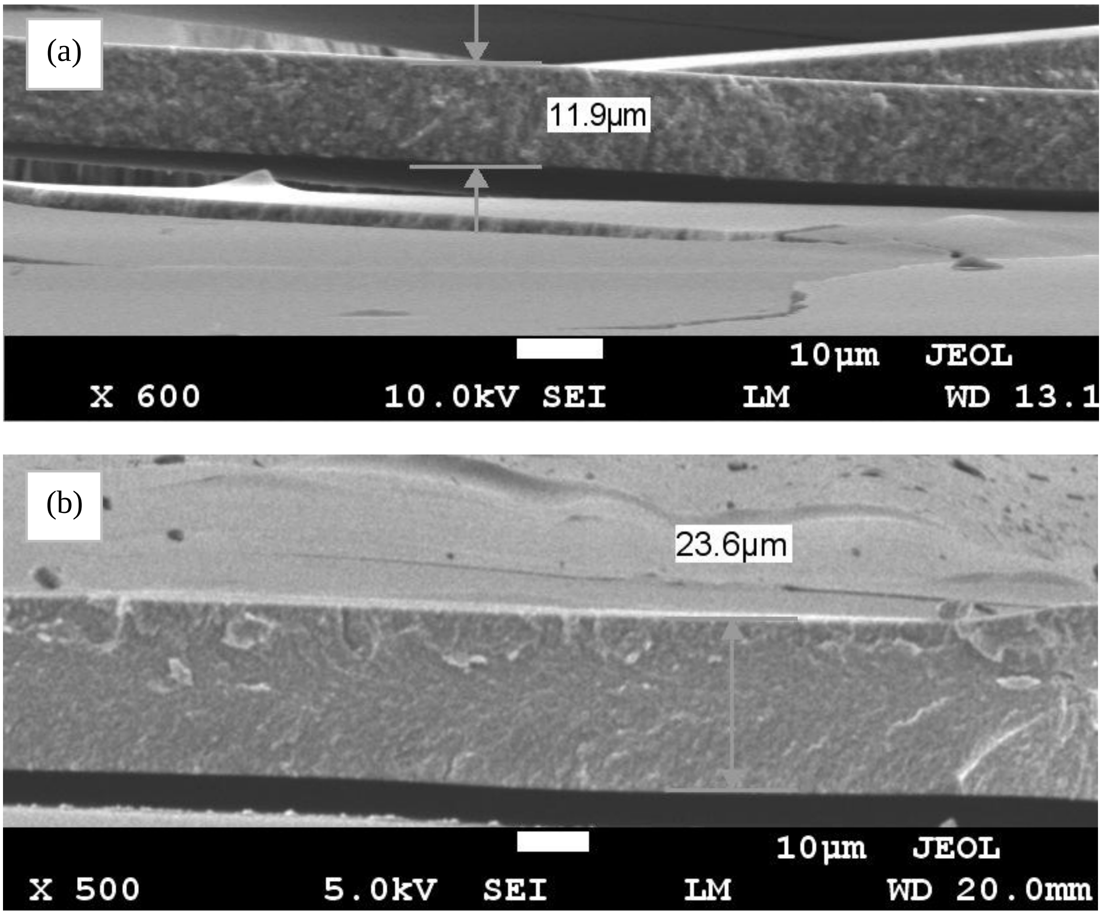

Figure 8.4. SEM images of TiO_2 layer thickness as prepared with doctor blade method on (a) one layer of Scotch tape, and (b) two layers of Scotch tape. The TiO_2 layer thickness is shown by the arrow with the value enclosed.

Besides surface passivation by ZnS and different TiO_2 film thickness, some groups applied chemical treatment on the TiO_2 film such as $TiCl_4$ [18,19]. The treatment of TiO_2 with $TiCl_4$ has been a practice in DSSC and it has a positive effect on the solar cell performance [20,21]. In this study, $TiCl_4$ treatment was performed according to Kim *et al.*'s work [18]. Briefly, the sintered TiO_2 electrode was immersed in a 40 mM $TiCl_4$ aqueous solution at 70°C for 30 minutes. Then the electrode was rinsed with DI water before sintered at 450°C for 30 minutes. The treatment with $TiCl_4$ will produce a thin TiO_2 coating layer on top of the existing TiO_2 nano-particles. As QDs may not cover the entire surface of the TiO_2 particle, this coating layer helps in suppressing the back electron transfer at the TiO_2/electrolyte interface. In CdS QDSSC, a $TiCl_4$ treatment on 24 μm thick TiO_2 produces an efficiency of 0.98%. It seems the chemical treatment does not boost the performance of the solar cell when compared to the cell with non-treated electrode. The reduction of the performance is largely attributed to the lower photocurrent density and fill factor although there is an increase in open-circuit voltage. The same effect is also observed in CdSe QDSSC where the efficiency is 1.81%. Again, the reduction of the performance is due to the lower photocurrent density and fill factor. Contrary to the reported result in the literature, the lower performance in this study signifies a higher back electron transfer at the photoanode/electrolyte interface. This could be due to the coating layer paving for additional recombination routes instead of passivating the TiO_2 film. When scattering layer was added to the $TiCl_4$-treated electrode, the performance of CdS QDSSC deteriorated further. Such cell obtained an efficiency of 0.57%. This indicates an even higher back electron transfer at the photoanode/electrolyte interface as explained previously. However, in CdSe QDSSC, the addition of scattering layer with $TiCl_4$-treated TiO_2 helps in boosting the performance of the solar cell. The $TiCl_4$-treated CdSe QDSSC with scattering layer and ZnS passivation layer has an efficiency of 2.55%. It has the highest photocurrent density compared to previous cells. However, due to lower open-circuit voltage and fill factor, its efficiency falls short compared to the cell with untreated TiO_2 and without scattering layer. This result implies that scattering layer may work well with thicker TiO_2 film sensitized with CdSe QD. The effect of scattering layer is manifested in this CdSe QDSSC as CdSe is a good light absorber compared to CdS. In short, a high solar cell performance can be obtained by just raising the thickness of TiO_2 layer to 24 μm and passivated by ZnS layer.

8.2.2 Effect of doping in QDSSC

In year 2012, a new approach for enhancing QDSSC performance was reported by Kamat *et al.* [22]. In their work, CdS/CdSe QD co-sensitized solar cell was doped with optically active transition metal ion, namely Mn^{2+}. This method has resulted in a dramatic improvement in the solar cell performance. In this work, Mn^{2+} doping was performed by mixing 0.075 M manganese acetate tetrahydrate into cadmium nitrate ethanolic solution. Then SILAR dipping was performed as per procedure outlined in Chapter 3. With the present of Mn^{2+}, it alters the charge separation and recombination process in the QD. An electronic state will be created in the midgap area of the QD. This causes the charge to stay longer before being recombined. As such, the charge will be transported to the TiO_2 instead [22]. A Mn-doped CdS QDSSC shows an efficiency of 1.68%, an increase of 58% from undoped CdS QDSSC. The corresponding solar cell performances are shown in Figure 8.5 and Table 8.3. With ZnS passivation layer, the performance is further enhanced with efficiency of 1.89%. Both photocurrent density and open-circuit voltage improved with Mn^{2+} doping. The high open-voltage circuit is largely driven by the effect of the dopant in the QDs. However, the effect of Mn^{2+} dopant in CdSe QDSSC is not positive as shown in Figure 8.6 and Table 8.4. CdSe QDSSC with Mn^{2+} dopant has efficiency of 1.29% compared to 1.41% in an undoped CdSe QDSSC. The doping effect does not increase the open-circuit voltage as expected even though there is an increase in photocurrent density. With ZnS passivation layer, the cell efficiency increased to 1.31%, which is very insignificant. The lower than expected result of Mn-doped CdSe QDSSC could be due to band gap alignment between the Mn^{2+} dopant and CdSe QD. In summary, doping with Mn^{2+} is beneficial for CdS QDSSC.

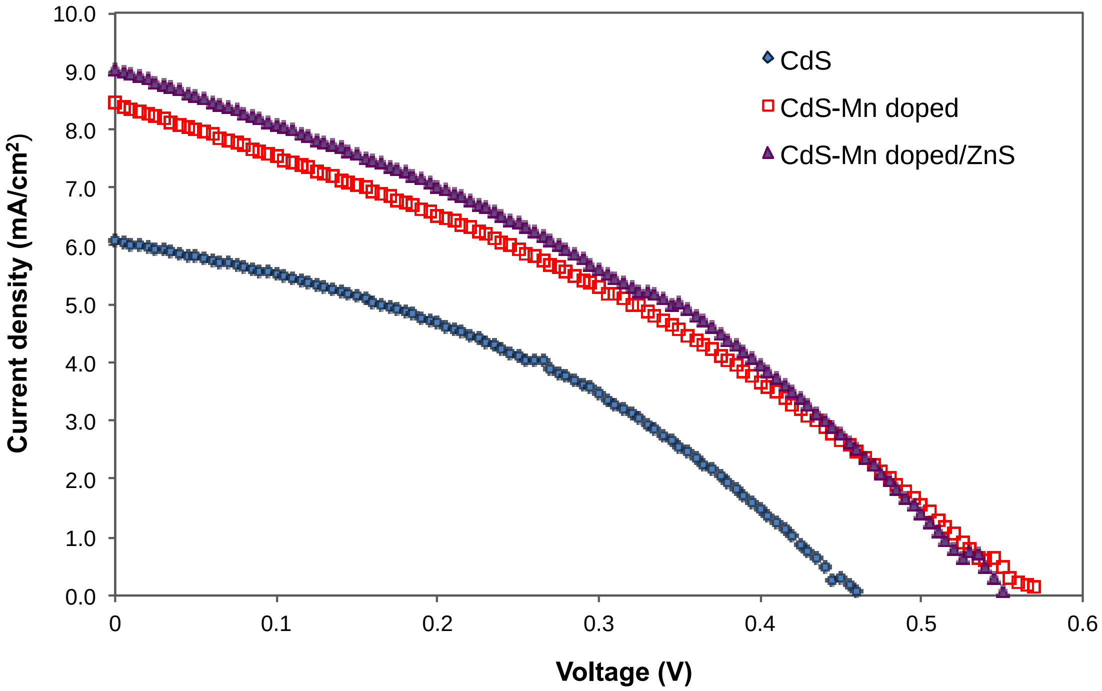

Figure 8.5. *J-V* curves of CdS QDSSCs with and without Mn-doped.

Table 8.3. Performance parameters of CdS QDSSCs with and without Mn-doped.

	Jsc (mA/cm^2)	V_{OC} (V)	FF (%)	η (%)
TiO_2/CdS – Mn doped	8.44	0.57	35.0	1.68
TiO_2/CdS – Mn doped/ZnS	9.05	0.55	38.0	1.89

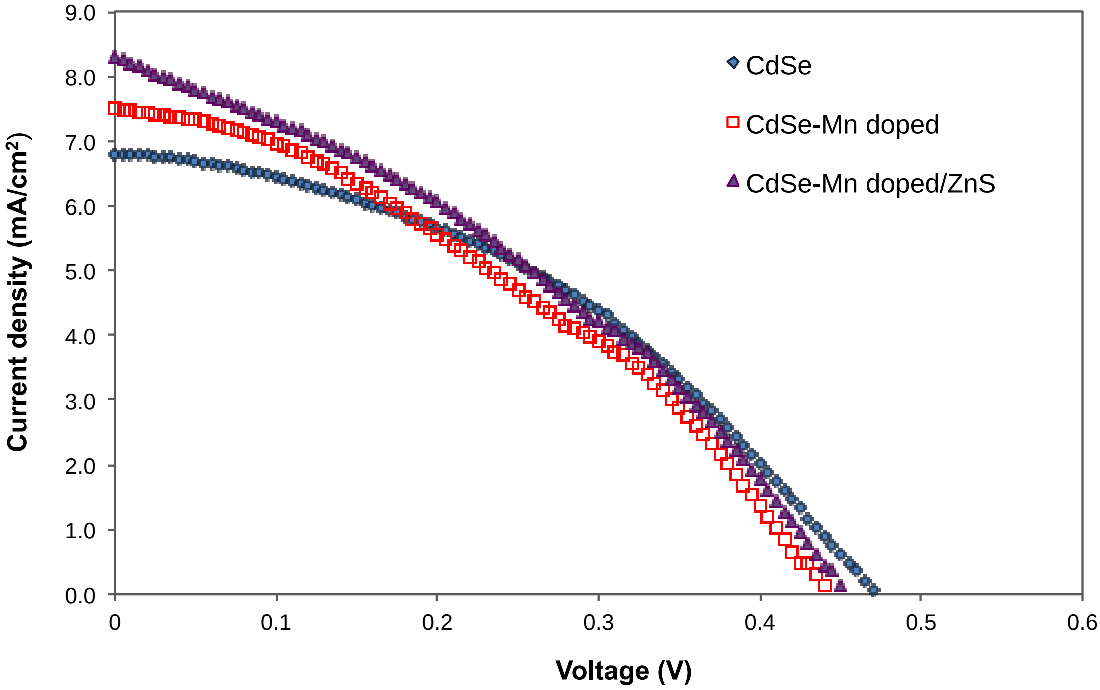

Figure 8.6. *J-V* curves of CdSe QDSSCs with and without Mn-doped.

Table 8.4. Performance parameters of CdSe QDSSCs with and without Mn-doped.

	Jsc (mA/cm^2)	V_{OC} (V)	FF (%)	η (%)
TiO_2/CdSe – Mn doped	7.49	0.44	39.0	1.29
TiO_2/CdSe – Mn doped/ZnS	8.31	0.45	35.0	1.31

8.3 Summary

Both CdS and CdSe QDSSC have been improved by altering the surface state or condition of the TiO_2 film. ZnS layer is beneficial for QDSSC as it functions as passivation layer by suppressing the charge recombination at the TiO_2/QD/electrolyte interface. By increasing the thickness of TiO_2 film, a higher cell performance was obtained. CdS and CdSe QDSSC with TiO_2 thickness of 24 μm have produced efficiency of 1.48% and 3.05%, respectively. Both cells have high photocurrent density where 8.43 mA/cm^2 was observed in CdS QDSSC and 14.16 mA/cm^2 in CdSe QDSSC. Doping with Mn^{2+} ion in QD is beneficial only in CdS QDSSC where a higher efficiency of 1.89% was obtained. The improved solar cells do not have major structure changes as illustrated in Figure 8.7. The alteration is only on the treatment of TiO_2/QD layer.

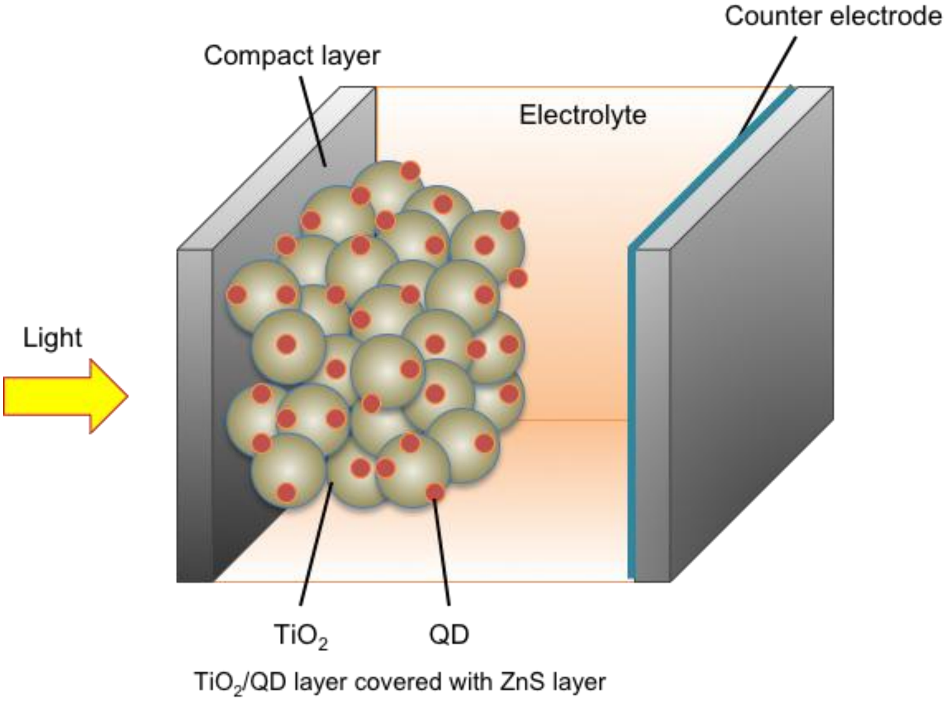

Figure 8.7. Structure of an efficient QDSSC.

8.4 References

[1] Mora-Sero, I., & Bisquert, J. (2010). Breakthroughs in the development of semiconductor-sensitized solar cells. *Journal of Physical Chemistry Letters, 1,* 3046-3052.

[2] Shen, Q., Kobayashi, J., Diguna, L.J., & Toyoda, T. (2008). Effect of ZnS coating on the photovoltaic properties of CdSe quantum dot-sensitized solar cells. *Journal of Applied Physics, 103,* 084304.

[3] Samadpour, M., Gimenez, S., Boix, P.P., Shen, Q., Calvo, M.E., Taghavinia, N., *et al.* (2012). Effect of nanostructured electrode architecture and semiconductor

deposition strategy on the photovoltaic performance of quantum dot sensitized solar cells. *Electrochimica Acta, 75,* 139-147.

[4] Hossain, M.A., Jennings, J.R., Shen, C., Pan, J.H., Koh, Z.Y., Matthews, N., *et al.* (2012). CdSe-sensitized mesoscopic TiO_2 solar cells exhibiting >5% efficiency: redundancy of CdS buffer layer. *Journal of Materials Chemistry, 22,* 16235-16242.

[5] Kim, J., Choi, H., Nahm, C., Kim, C., Nam, S., Kang, S., *et al.* (2012). The role of a $TiCl_4$ treatment on the performance of CdS quantum-dot-sensitized solar cells. *Journal of Power Sources, 220,* 108-113.

[6] Yang, S.-M., Huang, C.-H., Zhai, J., Wang, Z.-S., & Jiang, L. (2002). High photostability and quantum yield of nanoporous TiO_2 thin film electrodes co-sensitized with capped sulfides. *Journal of Materials Chemistry, 12,* 1459-1464.

[7] Guijarro, N., Campina, J.M., Shen, Q., Toyoda, T., Lana-Villarreal, T., & Gomez, R. (2011). Uncovering the role of the ZnS treatment in the performance of quantum dot sensitized solar cells. *Physical Chemistry Chemical Physics, 13,* 12024-12032.

[8] Li, Z.-X., Xie, Y.-L., Xu, H., Wang, T.-M., Xu, Z.-G., & Zhang, H.-L. (2011). Expanding the photoresponse range of TiO_2 nanotube arrays by CdS/CdSe/ZnS quantum dots co-modification. *Journal of Photochemistry and Photobiology A. Chemistry, 224,* 25-30.

[9] Grätzel, M. (2005). Solar energy conversion by dye-sensitized photovoltaic cells. *Inorganic Chemistry, 44,* 6841-6851.

[10] Wang, Z.-S., Kawauchi, H., Kashima, T., & Arakawa, H. (2004). Significant influence of TiO_2 photoelectrode morphology on the energy conversion efficiency of N719 dye-sensitized solar cell. *Coordination Chemistry Reviews, 248,* 1381-1389.

[11] Hore, S., Vetter, C., Kern, R., Smit, H., & Hinsch, A. (2006). Influence of scattering layers on efficiency of dye-sensitized solar cells. *Solar Energy Materials and Solar Cells, 90,* 1176-1188.

[12] Lee, J.-K., & Yang, M. (2011). Progress in light harvesting and charge injection of dye-sensitized solar cells. *Materials Science and Engineering: B, 176,* 1142-1160.

[13] Hagfeldt, A., Boschloo, G., Sun, L., Kloo, L., & Pettersson, H. (2010). Dye-sensitized solar cells. *Chemical Reviews, 110,* 6595-6663.

[14] Gao, F., Wang, Y., Shi, D., Zhang, J., Wang, M., Jing, X., *et al.* (2008). Enhance the optical absorptivity of nanocrystalline TiO_2 film with high molar extinction coefficient ruthenium sensitizers for high performance dye-sensitized solar cells. *Journal of the American Chemical Society, 130,* 10720-10728.

[15] Ito, S., Zakeeruddin, S.M., Humphry-Baker, R., Liska, P., Charvet, R., Comte, P., *et al.* (2006). High-efficiency organic-dye-sensitized solar cells controlled by nanocrystalline-TiO_2 electrode thickness. *Advanced Materials, 18,* 1202-1205.

[16] Lee, H.J., Bang, J., Park, J., Kim, S., & Park, S.-M. (2010). Multilayered semiconductor (CdS/CdSe/ZnS)-sensitized TiO_2 mesoporous solar cells: all prepared by successive ionic layer adsorption and reaction processes. *Chemistry of Materials, 22,* 5636-5643.

[17] Tian, J., Gao, R., Zhang, Q., Zhang, S., Li, Y., Lan, J., *et al.* (2012). Enhanced performance of CdS/CdSe quantum dot cosensitized solar cells via homogeneous distribution of quantum dots in TiO_2 film. *Journal of Physical Chemistry C, 116,* 18655-18662.

[18] Chi, C.-F., Chen, P., Lee, Y.-L., Liu, I.-Ping, Chou, S.-C., Zhang, X.-L., *et al.* (2011). Surface modifications of CdS/CdSe co-sensitized TiO_2 photoelectrodes

for solid-state quantum-dot-sensitized solar cells. *Journal of Materials Chemistry, 21*, 17534-17540.

[19] Zhao, F., Tang, G., Zhang, J., & Lin, Y. (2012). Improved performance of CdSe quantum dot-sensitized TiO_2 thin film by surface treatment with $TiCl_4$. *Electrochimica Acta, 62*, 396-401.

[20] Ito, S., Murakami, T.N., Comte, P., Liska, P., Grätzel, C., Nazeeruddin, M.K., *et al.* (2008). Fabrication of thin film dye sensitized solar cells with solar to electric power conversion efficiency over 10%. *Thin Solids Film, 516*, 4613-4619.

[21] Fan, S.-Q., Kim, C., Fang, B., Liao, K.-X., Yang, G.-J., Li, C.-J., *et al.* (2011). Improved efficiency of over 10% in dye-sensitized solar cells with a ruthenium complex and an organic dye heterogeneously positioning on a single TiO_2 electrode. *Journal of Physical Chemistry C, 115*, 7747-7754.

[22] Santra, P.K., & Kamat, P.V. (2012). Mn-doped quantum dot sensitized solar cells: A strategy to boost efficiency over 5%. *Journal of the American Chemical Society, 134*, 2508-2511.